Journal of Experimental and Applied Physics
Journal Homepage: jeap.ppj.unp.ac.id
Vol. 2, No. 4, December 2024.
ISSN (Print): 2988-0378 ISSN (Online): 2987-9256

Analysis of Normal Stress Distribution of Earthquakes in the Fault Segment of the West Sumatra Region using the Stress Inversion Method

Ellen Kurniawati Daya, Syafriani*, Hamdi, Harman Amir

Department of Physics, Universitas Negeri Padang, Padang 25131, Indonesia

Article History
Received : Dec, 18th 2024
Revised : Dec, 25th 2024
Accepted : Dec, 30th 2024
Published : Dec, 30th 2024

DOI:
https://doi.org/10.24036/jeap.v2i4.88

Corresponding Author
*Author Name: Syafriani
Email: syafri@fmipa.unp.ac.id

Abstract: West Sumatra, a highly earthquake-prone region, has five fault segments where normal stress distribution can reveal tectonic activity. This research used the stress inversion method to identify normal stresses, which could trigger or inhibit fractures. The data used involved 17 fault plane parameters (strike, dip, rake) from earthquakes with a magnitude of ≥4.7 that occurred in the West Sumatra region from 1967-2023. The type of fault analysed was strike-slip, and the earthquake's epicenter was located on land. The position of normal stress along the fault segment was illustrated using the pressure and tension axes (P/T), with respectively σ_1, σ_2, and σ_3 having azimuth/plunge values of 353.99°/4.76°, 247.26°/73.86°, and 85.31°/15.38°. The orientation of the highest normal stress (σ_1) is expanding towards the northern portion of the fault segment, meanwhile the intermediate normal stress (σ_2) is in the western region of the fault segment, and the lowest normal stress (σ_3) is found in the eastern part of the fault segment in this area. An analysis of the normal stress distribution shows that the Talamau segment is dominated by maximum normal stress, indicating that the Pasaman area and its surroundings are vulnerable to faults and earthquakes.

Keywords: Earthquake, Fault, Normal Stress, Stressinverse

1. Introduction

Indonesia, with a total land area of 1.92 x 10^6 km^2 and a water areas of 3.26 x 10^6 km^2, consists of 17,504 islands stretching from Sumatra to Papua [1]. Indonesia is highly susceptible to earthquake disasters due to its location at the convergence of three major tectonic plates: Eurasian, Pacific, and Indo-Australian. The interactions between these plates create pressure and displacement on faults throughout the region, both on land and on the seabed. For tens of millions of years, Indonesia has formed by merging various microcontinental plates and volcanic arcs, shaped by complex tectonic processes. The impact of the collision of these plates creates various

How to cite:
E. K Daya, Syafriani, Hamdi, H. Amir, 2024, Analysis of Normal Stress Distribution of Earthquakes in the Fault Segment of the West Sumatra Region using the Stress Inversion Method, *Journal of Experimental and Applied Physics,* Vol.2, No.4, page 119-130. https://doi.org/10.24036/jeap.v2i4.88

types of faults spread throughout Indonesia, receiving and storing tectonic forces from the current interaction of lithospheric plates [2].

Sumatra Island, located in Indonesia, is highly prone to seismic activity. Broadly, the tectonic framework of Sumatra comprises three primary systems. First, the downward motion of the Indo-Australian Plate beneath the Eurasian Plate creates a zone of subduction, bending the plate and forming an angular descent [3]. This process advances at an estimated rate of around ±50–60 mm annually [4]. The interaction at this boundary gives rise to the shallow subduction region referred to as the "Sumatra Megathrust Subduction". Second, the Sumatra Fault System, also referred to as "The Great Sumatra Fault," emerged due to substantial lateral forces generated by the oblique collision of the Indo-Australian Plate with the western edge of Sumatra Island. This fault moves at an average slip rate of around 14–15 mm/year [5]. The Sumatra Fault System consists of 19 primary segments [6]. Third, the Mentawai Fault System emerged because of oblique subduction near Sumatra Island. Stretching from south to north, the Mentawai Fault runs offshore along the Mentawai Islands and extends to the northern area of Nias [4].

West Sumatra ranks among the regions on Sumatra Island with significant earthquake vulnerability, largely due to the presence of five segments of the Sumatran Fault within its borders. These segments include the Sumpur segment (0.1 N to 0.3° N), the Sianok segment (0.7° S to 0.1° N), the Sumani segment (1.0° S to 0.5° S), the Suliti segment (1.75° S to 1.0° S), and the most recent addition, the Talamau segment [7,8]. Earthquakes occur when elastic strain energy in rocks is released due to the deformation of rocks in the lithosphere. This deformation is triggered by continuous pressure and pulls in the layers of the earth, causing rocks to reach their maximum elastic limit and experience sudden shifts or fractures [9]. The process by which significant and destructive earthquakes occur in an area needs to be understood through the accumulation of stress in the rocks around the fault.

A fault refers to a fracture zone characterized by the relative displacement of one rock block in relation to another. To identify the type of fault, certain parameters must be determined, including:

1. Strike (ϕ): This refers to the angle between the fault's strike line and the direction of north. It is measured in a clockwise direction from north to the strike of the fault, with a range from 0° to 360°.
2. Dip (δ): This represents the angle between the fault surface and a level horizontal plane. The dip is measured within a vertical plane that is perpendicular to the strike of the fault, with values varying between 0° and 90°.
3. Rake or Slip (λ): This describes the relative displacement of the hanging wall along the fault's strike. The values range from -180° to 180°, where positive values indicate an upward shift, and negative values indicate a downward shift.

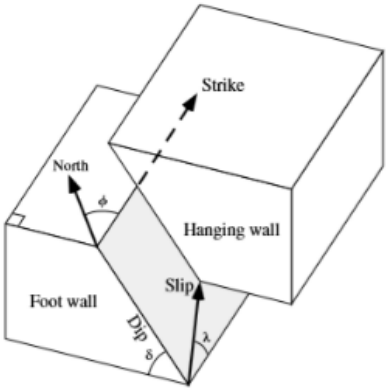

Figure 1. Strike, dip, and rake on faults [10]

Faults and slip directions can be oriented in various directions and are named relative to the orientation of the Earth's surface as seen in Figure 2.

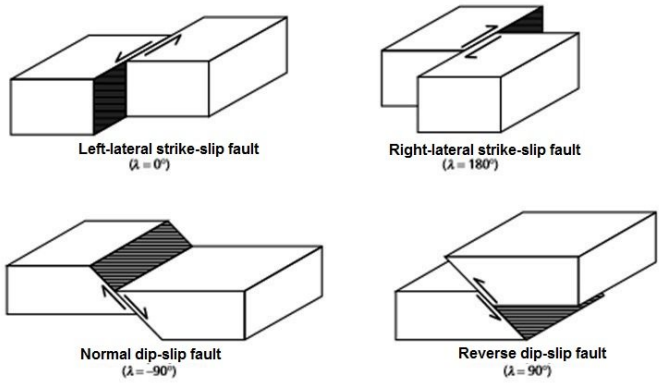

Figure 2. The basic orientation of the fault plane [11]

Stress accumulation in rocks surrounding a fault can be identified by examining stress tensor parameters, including the orientation and magnitude of normal stress. The parameters of this tensor are assessed by analyzing the distribution of normal stress on faults to pinpoint zones prone to fault activity and seismic events. The analysis of normal stress distribution is effectively conducted using the iterative stress inversion technique, which offers enhanced accuracy [12]. This method evaluates the stress state derived from multiple earthquake focal mechanisms, referencing Bott's hypothesis. According to this hypothesis, "a slip vector lies on the fault plane and corresponds with the highest shear stress resolvable on that plane" [13]. The inversion approach is based on Michael's methodology [14] and the instability criterion [15].

The stress inversion technique utilizes a formulation to determine normal traction and fault shear, denoted as σ_n and τ [14] :

$$\sigma_n = T_i n_i = \tau_{ij} n_i n_j \quad (1)$$

$$\tau N_i = T_i - \sigma_n n_i = \tau_{ij} n_j - \tau_{jk} n_j n_k n_i = \tau_{kj} n_j (\delta_{ik} - n_i n_k) \quad (2)$$

where **N** refers to the direction of the shear component τ and is located on the surface s. Next, Equation (2) is changed to:

$$\tau_{kj} n_j (\delta_{ik} - n_i n_k) = \tau N_i \quad (3)$$

As this method does not allow for the determination of the absolute stress value, τ is normalized to 1 in Equation (3). Equation (3) is then expressed in matrix form:

$$\boldsymbol{At} = \boldsymbol{s} \quad (4)$$

$$\boldsymbol{t} = [\, \tau_{11} \tau_{12} \tau_{13} \tau_{22} \tau_{23} \,]^T \quad (5)$$

A is a 3 x 5 matrix obtained through calculations of **n** normal faults, while s refers to the direction of the normalized slip vector.

Analyzing normal stress distribution based on fault plane parameters is one of the steps to mitigate earthquake risk. Information regarding the position and direction of maximum normal stress indicates that the region can be considered a fault-prone zone, with a high potential risk of earthquakes.

An examination of the distribution of normal stress along the Sumatran Fault was previously conducted using the stress inversion technique. The results indicated that the northern region, characterized by intense seismic activity, experienced the highest stress levels, moderate stress was observed near the fault, and the lowest stress levels were identified in the eastern region [16]. However, given the extensive scope of the study, covering 1,900 km from Banda Aceh to Teluk Semangko, a more detailed analysis is needed. Therefore, further research should focus on partitioning the Sumatran Fault into several sections, with one of these being the West Sumatra region.

2. Materials and Method

This research adopted a descriptive approach and relied on secondary sources, particularly fault plane characteristics (strike, dip, rake), sourced from the CMT IRIS earthquake catalog. This data focused on the nodal plane lines (NP1 and NP2) of the fault segment in the West Sumatra region during the period 1967-2023. Normal stress distribution was analyzed via the stress inversion method using STRESSINVERSE software. STRESSINVERSE is a Matlab or Python software, used to perform iterative inversions to determine stress and fracture orientations of focal mechanisms [17]. The data used was data on significant and destructive earthquakes with an earthquake strength of ≥4.7 magnitude that occurred in West Sumatra and its surroundings at coordinates 0.55ºN to -2.6ºS and 99.13º-101.81ºE. The amount of data obtained was chosen based on the type of fault that would be used, namely strike-slip fault. The data processing steps taken to determine the normal stress distribution were as follows:

First, the fault plane parameter data, which had been sorted based on the type of fault to be used, was input into the STRESSINVERSE package directory data box, and it was processed using the Matlab R2007b application. Second, after the data was input, the stress inversion stage was then carried out using Equation (7):

$$\boldsymbol{t} = \boldsymbol{A}^{-g} \boldsymbol{s} \quad (6)$$

This inversion process implemented fault instability constraints using Equation (7). Integrating fault instability boundaries into the inversion process led to the development of an iterative procedure [18].

$$I = \frac{\tau - \mu(\sigma - 1)}{\mu + \sqrt{1 + \mu^2}} \quad (7)$$

Third, analyzing the connection between normal stress (Tn) and shear stress (Tt) was performed using the Mohr circle diagram to estimate peak stress values based on Equation (8):

$$\begin{aligned} \left(T_n - \frac{\sigma_2 + \sigma_3}{2}\right)^2 + T_t^2 &\geq \left(\frac{\sigma_2 + \sigma_3}{2}\right)^2 \\ \left(T_n - \frac{\sigma_3 + \sigma_1}{2}\right)^2 + T_t^2 &\geq \left(\frac{\sigma_3 + \sigma_1}{2}\right)^2 \\ \left(T_n - \frac{\sigma_1 + \sigma_2}{2}\right)^2 + T_t^2 &\geq \left(\frac{\sigma_1 + \sigma_2}{2}\right)^2 \end{aligned} \quad (8)$$

The fourth step was to determine the distribution of the pressure and tension axes (P/T) with the position of the main stress. Next, the shape ratio of the histogram could be determined. Accurate values and shape ratios could be obtained through inversion iterations for stress and fracture orientations. Determining the accurate value of this shape ratio used the Equation (9):

$$R = \frac{\sigma_1 - \sigma_2}{\sigma_1 - \sigma_3} \quad (9)$$

Lastly, a graph illustrating the confidence bounds for the primary stress orientations was created, where each orientation corresponds to σ_1, σ_2, and σ_3. Examining how normal stress is distributed in terms of position and orientation can be used as a strategy to mitigate earthquake risks in West Sumatra Province, reducing potential damage and losses caused by seismic events.

3. Results and Discussion

This research produced various visualizations, including Mohr's circle diagrams, P/T axis graphs showing the positions of the main stresses on the focal sphere, shape ratio histograms, and images of the confidence limits for stress directions. These were derived from fault plane characteristics sourced from the IRIS Centroid Moment Tensor (CMT) catalog of seismic events. The study concentrated on 17 strike-slip fault earthquake events that occurred between 1967 and 2023, with epicenters situated on land. A beach ball distribution map, based on this earthquake data, illustrating fault segments in West Sumatra, is presented in Figure 3.

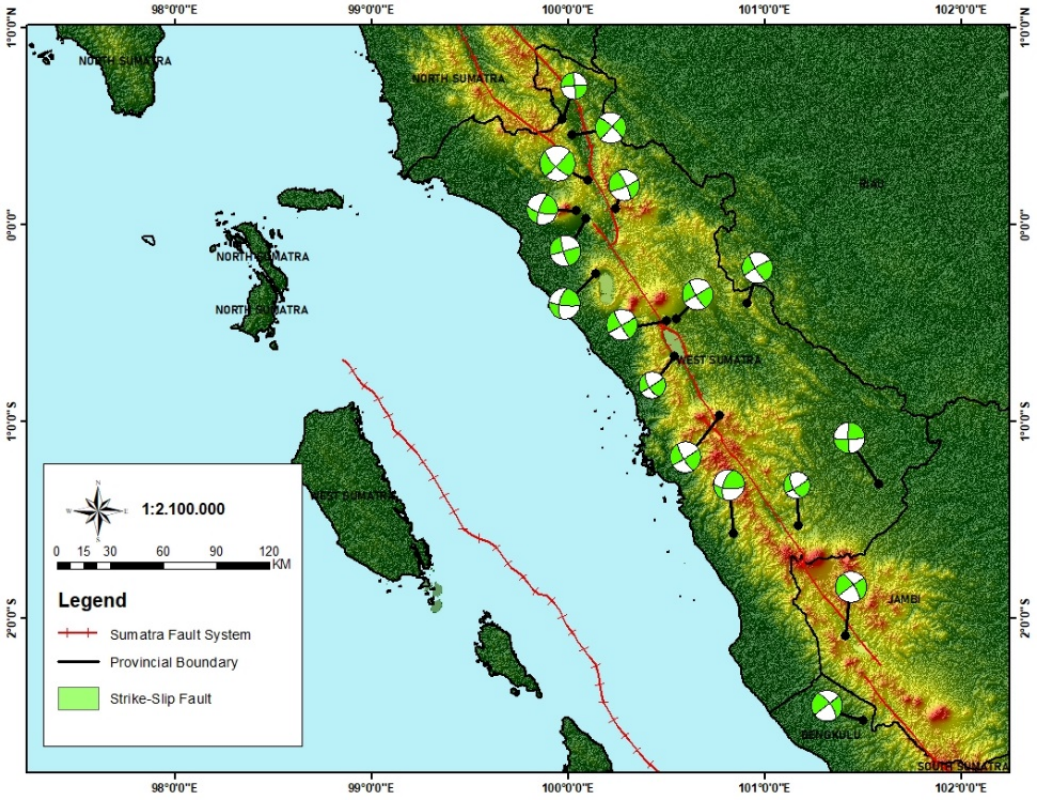

Figure 3. Earthquake Event with Strike-Slip Fault Type.

The fault plane parameter data from the 17 earthquake events can be seen in Table 1.

Table 1. Fault plane parameters (strike, dip, rake)

No.	Date-Time (UTC)	Nodal Plane I			Nodal Plane II		
		Strike (^{0})	Dip (^{0})	Rake (^{0})	Strike (^{0})	Dip (^{0})	Rake (^{0})
1	1977/03/08 23:17:28.0	312	80	179	42	89	10
2	1986/08/12 05:09:07.4	66	81	10	334	81	170
3	1995/10/06 18:09:45.9	326	74	-177	235	87	-16
4	2007/03/06 03:49:38.9	150	84	-177	60	87	-6
5	2007/03/06 05:49:26.9	149	80	179	239	89	10
6	2007/03/06 12:53:06.9	148	79	175	239	85	11
7	2008/11/10 08:58:50.5	192	62	12	97	79	152
8	2009/01/26 05:23:24.6	104	69	166	199	77	22
9	2009/09/19 10:50:44.9	355	86	-177	264	87	-4
10	2009/10/01 01:52:27.3	323	70	-178	232	88	-20
11	2014/09/10 17:46:19.2	148	67	-177	57	87	-23
12	2015/06/12 19:54:25.0	154	60	-168	57	79	-30
13	2016/07/10 09:31:56.7	164	80	-180	74	90	-10
14	2018/07/21 07:58:16.0	149	77	-176	58	86	-13
15	2019/02/27 23:27:04.2	88	81	174	179	84	9
16	2022/02/25 01:39:26.5	135	73	-175	44	85	-17
17	2023/03/01 23:05:23.4	197	60	24	94	69	147

(Source: [19])

Following processing with the stress inversion technique, the outcomes of this study included a Mohr's circle plot, a graph of the P/T axis with the position of the main stress on the focus sphere, a histogram of shape ratios, and an image of the confidence limit for the direction of the main stress.

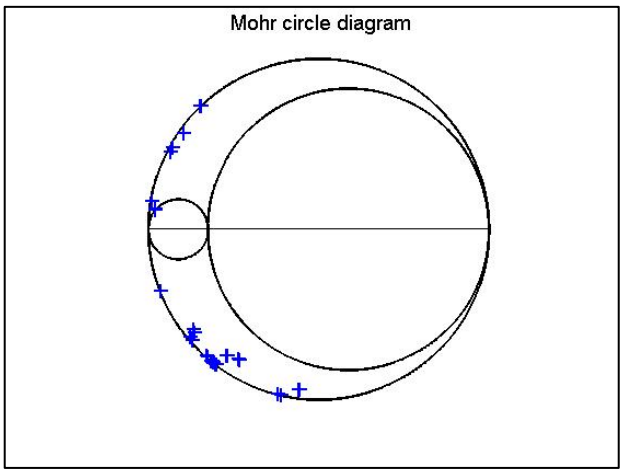

Figure 4. Mohr's Circle Diagram

Figure 4 explains that the interpretation of the graph produced by the Mohr diagram is useful for understanding the stress situation in a material. The outermost circle, containing the blue dot, represents the main fault plane within the C2 solution region (according to Equation 8), which indicates the Mohr failure solution area of the other two circles. The blue marker (blue plus sign) on the Mohr diagram indicates the primary fault plane that is most favorably aligned with stress. Planes of faulting situated in the top and bottom sections trigger conjugate faults, which are arranged in a balanced manner relative to the principal compressive force [20]. These conjugate faults, which meet at a point within the Earth's crust, are highly unstable and closely parallel to the main fault.

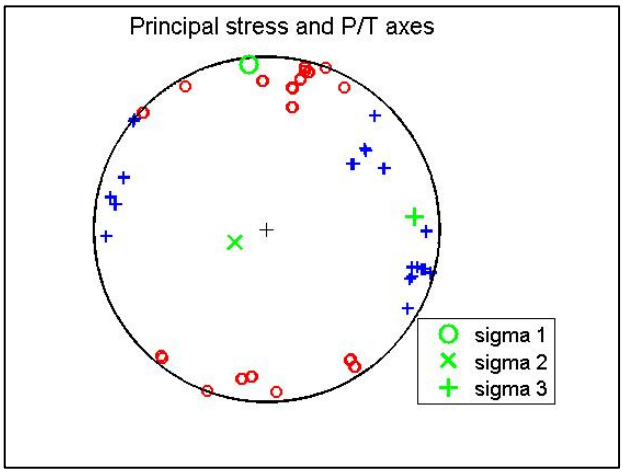

Figure 5. Distribution of P/T Axis with Main Stress Position

Figure 5 illustrates the alignment of the P/T axis with the direction of the principal stress. These axes are differentiated using two colors, namely red and blue. The red color is used to indicate pressure or the P axis, while the blue color is used to depict stress or T axis. The image provides information that aligns with the direction of the main stress. The green circle symbolizes σ_1, the green cross denotes σ_2, and the green plus sign represents σ_3.

The alignment of the primary fault plane is strongly influenced by both the stress and fault friction. The distribution of the P/T axis in Figure 5 reflects the predominant fault type in the Sumatra fault zone area, specifically right-lateral strike-slip (dextral). The P/T axis is positioned within the σ_1 and σ_3 planes. The location of σ_1 is at the center of the P axis, while σ_3 is situated at the center of the T axis. Nodal planes of principal faults are characterized by a deviation or tilt angle of less than 45° relative to the σ_1 direction [21]. The P/T axis forms two separate sub-clusters, commonly referred to as the "butterfly wings" pattern, which emphasizes the precision of the focal mechanism and stress uniformity. Increased friction leads to a wider separation of the wings, whereas reduced friction or higher pore pressure causes them to converge or even overlap.

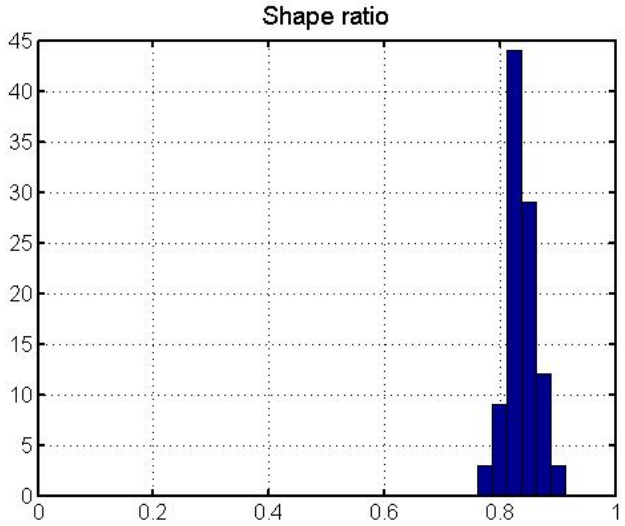

Figure 6. Shape Ratio Histogram

Figure 6 illustrates stress accuracy based on the shape ratio, which is determined through repeated joint inversion of stress and fracture orientations. However, incorrect faults in plane selection significantly reduces its accuracy. The shape ratio histogram, sensitive to the inversion mechanism and its precision, in this study approaches 0.9 within the theoretical range of 0.7 to 1 [12]. This confirms the consistency of the research findings with established theoretical principles.

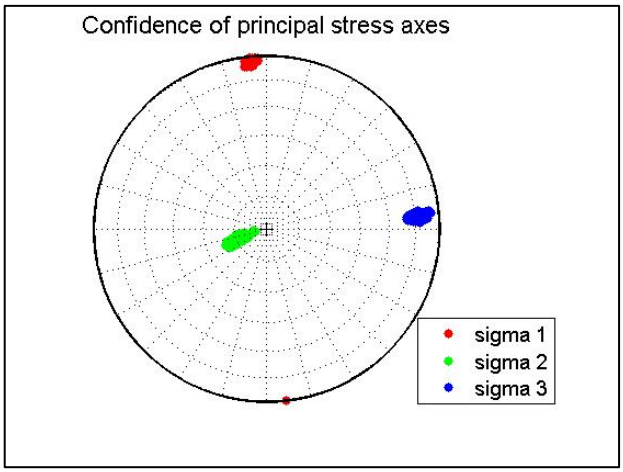

Figure 7. Confidence Limits of Principal Stress Direction

Figure 7 illustrates confidence bounds for the directions of principal stress, marked by points corresponding to each stress component. The red point (representing maximum normal stress, σ_1) highlights significant seismic activity in the northern section of the fault in West Sumatra. The green point (indicating intermediate normal stress, σ_2) is located to the west of the fault segment, while the blue points (denoting minimum normal stress, σ_3) are positioned to the east of the fault segment in the same area.

Table 2. Results of Stress Inversion Parameters (Stress)

σ_1 Azimuth/Plunge (°)	σ_2 Azimuth/Plunge (°)	σ_3 Azimuth/Plunge (°)	R
353.99°/4.76°	247.26°/73.86°	85.31°/15.38°	0.83 ± 9.84%

Table 2 displays the results of the stress inversion, with the maximum normal stress (σ_1) occurring at an azimuth of 353.99° and a plunge of 4.76°, the intermediate normal stress (σ_2) at an azimuth of 247.26° and a plunge of 73.86°, and the minimum normal stress (σ_3) at an azimuth of 85.31° and a plunge of 15.38°. Azimuth is defined as the angle measured clockwise from 0° (north) to 360°, while plunge refers to the angle between a line and the horizontal plane, ranging from 0° to 90°. The R shape ratio is 0.83, with an average error of 9.84%, which remains below the 10% accuracy threshold [12].

The Sumatra Fault System is a key strike-slip fault that facilitates dextral motion and the convergence of the Indo-Australian and Eurasian tectonic plates. As the subduction zone moves northward in a clockwise direction, the rate of dextral displacement along the fault is believed to increase toward the northern areas [22].

The analysis of normal stress distribution in the West Sumatra fault segments reveals that the maximum normal stress is concentrated around the Sumpur segment (0.1 N to 0.3° N), the Sianok segment (0.7° S to 0.1° N), and Talamau segments. The Talamau segment, located in the Pasaman area in northern West Sumatra, is a newly formed fault resulting from the Mw 6.1 earthquake on February 25, 2022. This earthquake, caused by a blind fault an undetectable fault that doesn't reach

the surface triggered a landslide on Mount Talamau [8]. An evaluation of seismic hazard potential, incorporating fault characteristics and coseismic stress from the Pasaman event, suggests a high likelihood of rupture for all the fault zones involved [23].

The maximum detected normal stress in the Sumpur, Sianok, and Talamau segments reflects a significant concentration of tectonic pressure, indicating a high potential for deformation or large earthquakes in this region. Furthermore, the data indicates that the Talamau segment, being a newly formed fault, presents a significant seismic risk due to its connection with a blind fault. The prevailing intermediate stress (σ_2) near the fault and the lowest stress (σ_3) in the eastern region reveal a pressure distribution pattern that aids in understanding the tectonic behavior of the area, including forecasts of fault activity and interactions between segments.

This study also highlights the contribution of subduction to the increased dextral slip rate to the north of the Sumatra Fault, suggesting that the northern region is at a higher risk of large-magnitude earthquakes. The shape ratio (R) of 0.83 with an error margin of less than 10% reinforces the accuracy of this analysis and provides additional insight into the dominant forces at play in the region.

The results of this study provide important insights into how normal stress is distributed in regions with significant seismic activity. These insights are essential for reducing disaster risks, particularly in reinforcing infrastructure, identifying landslide hazards, and improving community readiness, especially in the Pasaman area and surrounding segments. Furthermore, further analysis of cosmic stress and changes in fault behaviour can provide a deeper understanding to reduce the potential for aftershocks.

4. Conclusion

The pressure and tension axes (P/T) represent the normal stress distribution in the West Sumatra fault segments. Maximum normal stress (σ_1) occurs at an azimuth of 353.99° with a plunge of 4.76°, intermediate normal stress (σ_2) at an azimuth of 247.26° with a plunge of 73.86°, and minimum normal stress (σ_3) at an azimuth of 85.31° with a plunge of 15.38°. The maximum stress (σ_1) is directed north of the fault segment, intermediate stress (σ_2) west, and minimum stress (σ_3) east. The analysis identifies the Talamau segment as dominated by maximum normal stress, making the Pasaman area and its surroundings highly susceptible to faults and earthquakes.

Acknowledgments

The author would like to thank IRIS has providing and continuing to update the CMT (Centroid Moment Tensor) data catalog that the author has used in this research. The author also thanks Václav Vavryčuk for providing the software Stress inverse along with the guidebook that has been provided to expedite this research process.

References

[1] J. T. Simamora and E. L. Namigo, "Pemetaan Magnitude of Completeness (Mc) untuk Gempa Sumatera," *J. Fis. Unand*, vol. 5, no. 2, pp. 179–186, 2016, doi: 10.25077/jfu.5.2.179-186.2016.

[2] S. Husein, "Bencana Gempabumi," *DRR Action Plan Work. Strengthened Indones. Resil. Reducing*

Risk from Disasters, pp. 1–10, 2015.

[3] Akmam, L. Dwridal, and B. M. Kemal, "Studi Karakteristik Fisis Sumber Gempabumi di Wilayah Sumatera Barat," 2006.

[4] R. Triyono, "Ancaman Gempa Bumi Di Sumatera Tidak Hanya Bersumber Dari Mentawai Megathrust," pp. 1–23, 2016.

[5] K. E. Bradley, L. Feng, E. M. Hill, D. H. Natawidjaja, and K. Sieh, "Implications of the diffuse deformation of the Indian Ocean lithosphere for slip partitioning of oblique plate convergence in Sumatra," *J. Geophys. Res. Solid Earth*, vol. 122, no. 1, pp. 572–591, 2017, doi: 10.1002/2016JB013549.

[6] H. Amir *et al.*, "Subsurface structure of Sumani segment in the Great Sumatran Fault inferred from magnetic and gravity modeling," *Tectonophysics*, vol. 821, no. November, p. 229149, 2021, doi: 10.1016/j.tecto.2021.229149.

[7] F. D. Raharjo, A. Z. Sabarani, M. J. Fisika, S. Pengajar, and J. Fisika, "Analisis Variasi Spasial Parameter Seismotektonik Daerah," *Pillar Phys.*, vol. 8, pp. 73–80, 2016.

[8] B. G. Dewanto *et al.*, "The 2022 Mw 6.1 Pasaman Barat, Indonesia Earthquake, Confirmed the Existence of the Talamau Segment Fault Based on Teleseismic and Satellite Gravity Data," *Quaternary*, vol. 5, no. 45, pp. 1–19, 2022, doi: 10.3390/quat5040045.

[9] L. Linda, N. Ihsan, and P. Palloan, "Analisis Distribusi Spasial Dan Temporal Seismotektonik Berdasarkan Nilai B-Value Dengan Menggunakan Metode Likelihood Di Pulau Jawa," *J. Sains dan Pendidik. Fis.*, vol. 15, no. 1, pp. 16–31, 2019, doi: 10.35580/jspf.v15i1.9403.

[10] N. N. S. K. Wardani, K. N. Suarbawa, and R. Kusnandar, "Determination of Fault Type of Lombok Earthquakes from July 1 to December 31, 2018, using Focal Mechanism Method," *Bul. Fis.*, vol. 22, no. 2, p. 91, 2021, doi: 10.24843/bf.2021.v22.i02.p06.

[11] J. N. Mohamad, "Penentuan Arah Patahan Yang Terdapat Di Pulau Timor Dan Sekitarnya Menggunakan Mekanisme Sumber 3d Gempabumi," *J. Fis. Fis. Sains dan Apl.* , vol. 1, pp. 52–57, 2016.

[12] V. Vavryčuk, "Iterative joint inversion for stress and fault orientations from focal mechanisms," *Geophys. J. Int.*, vol. 199, no. 1, pp. 69–77, 2014, doi: 10.1093/gji/ggu224.

[13] S. Q. Jia, D. W. Eaton, and R. C. K. Wong, "Stress inversion of shear-tensile focal mechanisms with application to hydraulic fracture monitoring," *Geophys. J. Int.*, vol. 215, no. 1, pp. 546–563, 2018, doi: 10.1093/gji/ggy290.

[14] A. J. Michael, "Determination Of Stress From Slip Data: Faults And Folds," vol. 89, pp. 517–526, 1984.

[15] B. Lund and R. Slunga, "Stress tensor inversion using detailed microearthquake information and stability constraints: Application to Ölfus in southwest Iceland," *J. Geophys. Res. Solid Earth*, vol. 104, no. B7, pp. 14947–14964, 1999.

[16] W. Rahmawati and Madlazim, "Analisis Distribusi Tegangan Normal Gempa Bumi Di Wilayah Sesar Sumatra Menggunakan Metode Inversi Tegangan," *Inov. Fis. Indones.*, vol. 10, no. 2, pp. 73–80, 2021.

[17] V. Vavryčuk, "Stressinverse User Guide," 2020.

[18] V. Vavryčuk, F. Bouchaala, and T. Fischer, "High-resolution fault image from accurate locations and focal mechanisms of the 2008 swarm earthquakes in West Bohemia, Czech

Republic," *Tectonophysics*, vol. 590, pp. 189–195, 2013, doi: 10.1016/j.tecto.2013.01.025.

[19] G. Ekström, M. Nettles, and A. M. Dziewoński, "The global CMT project 2004-2010: Centroid-moment tensors for 13,017 earthquakes," *Phys. Earth Planet. Inter.*, vol. 200–201, pp. 1–9, 2012, doi: 10.1016/j.pepi.2012.04.002.

[20] L. Fojtíková and V. Vavryčuk, "Tectonic stress regime in the 2003–2004 and 2012–2015 earthquake swarms in the Ubaye Valley, French Alps," *Pure Appl. Geophys.*, vol. 175, no. 6, pp. 1997–2008, 2018, doi: 10.1007/s00024-018-1792-2.

[21] V. Vavryčuk, "Principal earthquakes: Theory and observations from the 2008 West Bohemia swarm," *Earth Planet. Sci. Lett.*, vol. 305, no. 3–4, pp. 290–296, 2011, doi: 10.1016/j.epsl.2011.03.002.

[22] D. H. Natawidjaja, "Updating Active Fault Maps and Sliprates Along the Sumatran Fault Zone, Indonesia," *IOP Conf. Ser. Earth Environ. Sci.*, vol. 118, no. 1, 2018, doi: 10.1088/1755-1315/118/1/012001.

[23] R. Wulandari, C. H. Chan, and A. Wibowo, "The 2022 Mw6.2 Pasaman, Indonesia, earthquake sequence and its implication of seismic hazard in central-west Sumatra," *Geosci. Lett.*, vol. 10, no. 1, 2023, doi: 10.1186/s40562-023-00279-6.